ChemComm

Accepted Manuscript

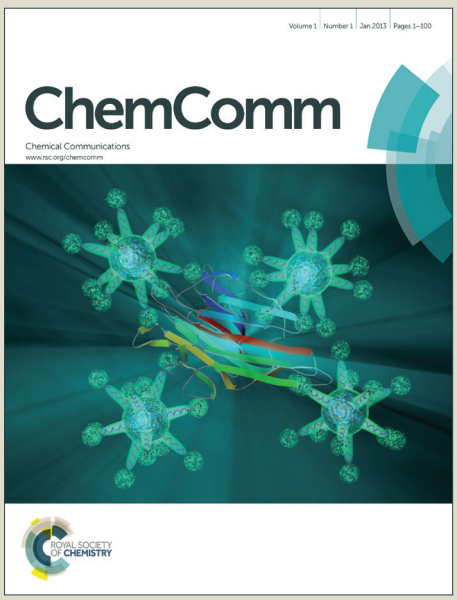

ROYAL SOCIETY OF CHEMISTRY

www.rsc.org/chemcomm

Journal Name

RSCPublishing

COMMUNICATION

N-doped microporous carbons derived from direct carbonization of K^+ exchanged meta-aminophenol-formaldehyde resin for superior CO_2 sorption

Cite this: DOI: 10.1039/x0xx00000x

Received ooth January 2012,
Accepted ooth January 2012

DOI: 10.1039/x0xx00000x

www.rsc.org/

Jin Zhou,[a] Zhaohui Li,[a] Wei Xing,[b*] Tingting Zhu,[a] Honglong Shen,[a] and Shuping Zhuo[a*]

N-doped microporous carbons with uniform ultramicropores (~0.50 nm) are facilely prepared by direct carbonization of K^+ exchanged meta-aminophenol-formaldehyde resin. These materials give an unprecedented CO_2 uptake of 1.67 mmol g^{-1} at 25 °C and 0.15 bar and superior CO_2-over-N_2 selectivity (50:1).

Global warming is one of most serious problems that human faces because it could cause a significant climate change. The IPCC (Intergovernmental Panel on Climate Change) has stated that the largest driver of global warming is carbon dioxide (CO_2) emissions from fossil fuel combustion, cement production, and land use changes such as deforestation. Thus, great efforts have been devoted to CO_2 abatement[1, 2]. Current technologies through the use of aqueous amines are being implemented to absorb CO_2. However, these methods are proven to be energy-costly and chemically inefficient. Up to now, physisorption of CO_2 using porous materials holds great promise due to its facile regeneration process.

In the past decade, various types of porous solid adsorbents including zeolite[3], metal-organic frameworks (MOFs)[4-6], porous carbon materials[7-11] and porous organic frameworks[12] have been studied for CO_2 capture. Among them, MOFs and porous carbon materials have gained most attention. Although MOFs exhibit excellent CO_2 capacities, these materials are water sensitive, and their preparation is more consuming and costly in comparison to the synthesis of porous carbons. Porous carbons are regarded as promising adsorbents due to their specific features such as low price, high specific surface area, hydrophobic surface, excellent thermal and chemical stability, and low energy requirements for regeneration.

It has been widely accepted that CO_2 sorption capacity is not determined by the total pore volume, but the volume of small micropores (<1.0 nm).[11, 13] Gogotsi and his co-workers reported that the pores smaller than 0.8 nm contributed the most to CO_2 uptake capacity on carbide derived carbons (CDCs) at 1 bar and pores small or equal to 0.5nm worked at 0.1 bar.[11] Our group further reported that pores smaller than 0.54 nm determine CO_2 sorption capacity at 0.15 bar (This pressure is a typical partial pressure of CO_2 in flue gases which is one of biggest sources of CO_2)[14]. Previous researches proposed a basic principle for designing highly efficient porous carbon adsorbents, that is, the porous carbons should primarily rich in ultramicropores, especially for CO_2 capture at low partial pressure. However, most of activated carbon materials show wide pore size distribution (PSD) and contain substantial supermicropores (larger than 1.0 nm), resulting in low CO_2 uptake, especially at low partial pressures (e.g. CO_2 capture from flue gas). On the other hand, it is also generally accepted that the introduction of nitrogen-containing groups into carbon framework can selectively improve the adsorption towards CO_2 over N_2.[7, 15, 16] Doping with nitrogen would also enhance the CO_2 adsorption capability of carbon materials, especially at low CO_2 partial pressures like in the case of flue gas.

Keeping the above factors in mind, herein, we report a new strategy to prepare N-doped microporous carbons (NMCs) with uniform ultramicropores (~0.50 nm) by direct carbonization of K^+ exchanged meta-aminophenol-formaldehyde resin. The as-prepared carbons can afford a high CO_2 uptake of 4.0 mmol g^{-1} at 25 °C and 1 bar. Of particular note is that these carbons exhibit an unprecedented CO_2 uptake of 1.67 mmol g^{-1} at 25°C and 0.15 bar and an impressive CO_2-over-N_2 selectivity (50:1).

The synthesis route of the NMCs is illustrated in Scheme 1. Firstly, dark red resin hydrogel was prepared by the aqueous polycondensation of meta-aminophenol and formaldehyde using equimolar KOH as a catalyst. After curing, the hydrogel was immersed in acetone for three days in which fresh acetone were replaced daily. The washed hydrogels are dried under flow air to give dark red xerogels (Fig. S1). Finally, the N-doped microporous carbons (NMC-*x*, where *x* designates

carbonization temperature in °C) are obtained by directly carbonizing these resin xerogels.

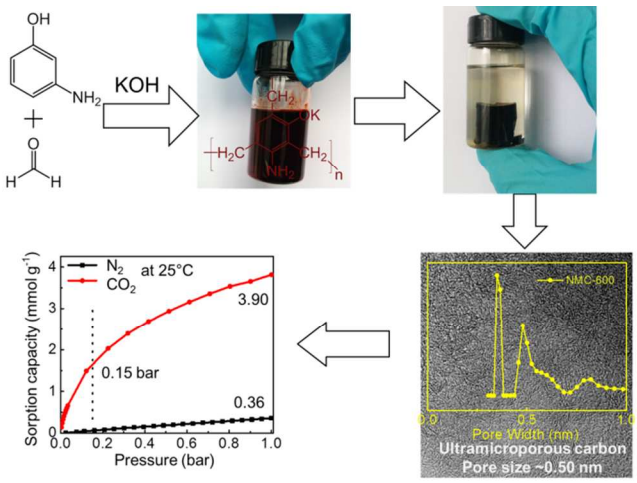

Scheme 1 Illustration of NMC-*x* for CO_2 sorption

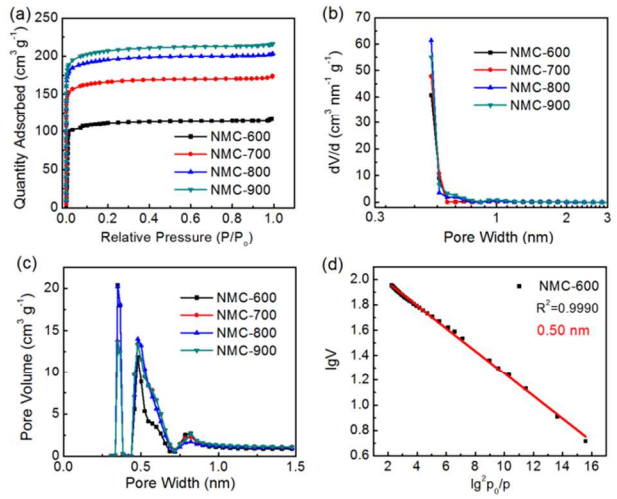

Fig. 1 (a) nitrogen sorption isotherms, (b) QSDFT pore size distributions derived from N_2 sorption, (c) NLDFT pore size distributions derived from CO_2 sorption, (d) D-R plots for CO_2 sorption by NMC-600

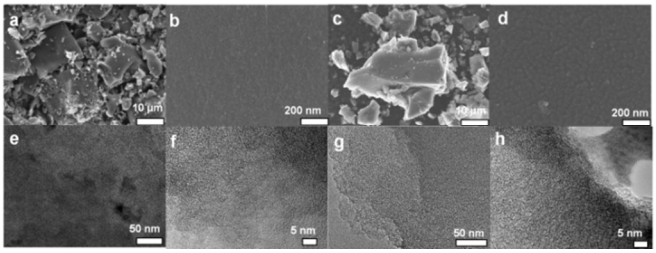

Fig. 2 SEM images of (a, b) NMC-600 and (c, d) NMC-900; TEM images of (e, f) NMC-600 and (g, h) NMC-900

The textural properties of the NMC-*x* were analysed by means of N_2 sorption at -196°C and CO_2 adsorption at 0 °C. It could be seen that all the NMC-*x* samples exhibit a standard type I isotherm with a narrow knee at a very low relative pressure (p/p^0<0.02) and an absence of apparent adsorption increment in the relative pressures over 0.02, which indicate that the porous carbons have a narrow micropore size distribution and that no mesopores are present. This is confirmed by the PSD plots obtained using quenched solid density functional theory (QSDFT) method (Fig. 1b)[17]. The specific surface area of NMC-*x* increases gradually from 272 m^2 g^{-1} to 664 m^2 g^{-1} as the activation temperature increases (Table S1). The values of specific surface areas are very close to the micropore surface area deduced from the t-plot method, which further demonstrates the microporous nature of NMC-*x*. PSD plots derived from CO_2 sorption using nonlocal density functional theory (NLDFT) methods also suggest that NMC-*x* contains abundant ultramicropores. The CO_2 Dubinin−Radushkevich (D-R) plots provide instructive information about the size of these ultramicropores (<0.8 nm). D-R plots of CO_2 sorption on NMC-*x* exhibit well-defined linear shapes (Fig. 1d, S2), showing that the porosity of NMC-*x* is made up of uniform ultramicropres[18, 19]. The average size of these ultramicropores calculated according to the slope of the D-R plots gradually increases from 0.50 to 0.58 nm as the activation temperature increases (Table S1). It could be observed that the pore volume obtained from the CO_2 sorption data is even larger than the total pore volume calculated from the N_2 sorption data, especially for NMC-600, also indicating the presence of extremely small micropores that may be hard to be accessible for N_2 molecules at cryogenic temperature[20].

The morphology and pore texture of NMC-*x* are further studied by scanning electron microscope (SEM) and transmission electron microscope (TEM) techniques (Fig. 2). It can be seen that the surface of NMC-*x* is smooth and compact without any clear pores. High resolution TEM (HRTEM) images clearly exhibit worm-like micropores for NMC-*x*. The potassium ions (K^+) mono-dispersed in resin xerogels as a form of $-O^-K^+$ play a key role in the formation of such a highly uniform ultramicropores. During the preparation, K^+ ion can exchange with H^+ in the hydroxyl groups, leading to atomic dispersion of K^+ ions in the bulk of phenolic resin. During the following carbonization step, the high dispersion of K^+ ions results in homogeneous and efficient chemical activation. This process does not require the input of an additional activating agent.

The crystalline structures of NMC-*x* are investigated by X-ray diffraction (XRD). No sharp peaks are present in their XRD patterns (Fig. S3), demonstrating the characteristic of amorphous carbon. Two broad diffraction bands centred at 23.4° and 43° can be approximately indexed as (002) and (101) plane of graphite structure. Raman spectra show well-resolved G and D bands centred at 1589 and 1340 cm^{-1}, which are the reflection of ideal and disordered graphitic lattice, respectively. The low value of I_G/I_D (about 1.2) further reflects the amorphous nature of NMC-*x*.

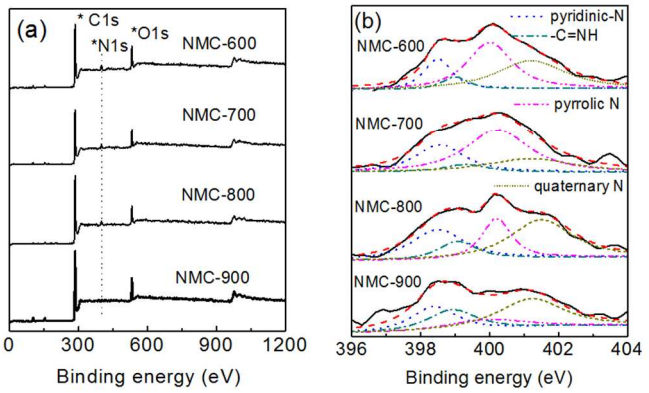

Fig. 3 (a) XPS spectra, (b) N1s of NMC-x

In order to confirm the N-doping of NMC-*x*, X-ray photoelectron spectroscopy (XPS), energy dispersive spectroscopy (EDS) and element analyses (EA) are conducted. The N content of NMC-*x* decreases as the activation temperature increases, and is determined to be 2.3-6.33 wt% and 1.3-3.8 at% by the EA and XPS measurements (Table S2, S3), respectively. The distributions of C, N and O in NMC-600 are homogeneous, as was confirmed by EDS mapping (Fig. S4). Four types of N-containing groups could be verified on the surface of the carbons, including pyridinic N, -C=NH, pyrrolic N and quaternary N, corresponding to the peaks at 398.2, 399.0, 400.5 and 401.0 eV, respectively (Fig. 3, Table S2). This N-doping is responsible for an increase in the surface polarity of carbon, and has been proved to improve CO_2 adsorption capacity at low partial pressure (like in the case of flue gas) and selectivity of CO_2 over N_2.[16, 21]

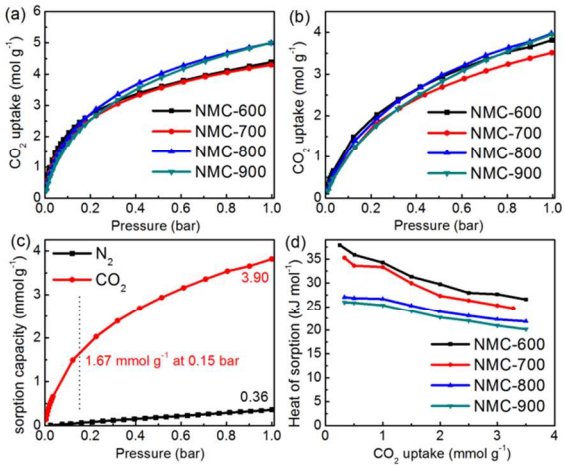

Fig. 4 (a) CO_2 sorption at 0 °C, (b) CO_2 sorption at 25 °C, (c) CO_2 and N_2 adsorption on NMC-600 at 25 °C , and (d) heats of adsorption

In consideration of their charecteristics such as microporoous and N-doped, we focus on the CO_2 sorption performance of NMC-*x*. CO_2 sorption isotherms of the NMC-*x* are measured at both 0 and 25 °C (Fig. 4). The NMC-*x* present high CO_2 uptakes, within the ranges of 4.4-5.1 mmol g^{-1} at 0 °C and 3.6-4.0 mmol g^{-1} at 25 °C (Table S4). Based on a recent review about CO_2 uptake on MOFs, our values are higher than most MOFs,[4] like Zn/DOBDC,[22] YO-MOF,[23] and bio-MOF-11.[5] In particular, NMC-600 exhibits an unprecedentedly high CO_2 capacity of 1.67 mmol g^{-1} at 25 °C under a low pressure of 0.15 bar, which corresponds to about 4 CO_2 molecules per nm^2. To the best of our knowledge, this is much higher than most of the reported carbon materials for capturing CO_2 under identical conditions (Table S5).[7-11, 13, 15, 16, 20, 24-30] We also carried out the CO_2 sorption measurement at elevated temperatures, such as 30, 50 and 75 °C (Fig. S5). It can be seen that the CO_2 uptake decreases significantly as the adsorption temperature increases because the molecular kinetic energy of CO_2 rises with increasing temperature. At 75 °C and 1 bar, the NMC-800 carbon still shows a very high CO_2 uptake of 2.0 mmol g^{-1}. To probe their selectivity of CO_2 over N_2, the CO_2 uptake was compared to N_2 uptake at 25 °C (Fig. 4c). At 25 °C and 1 bar, CO_2 uptake on NMC-600 (3.90 mmol g^{-1}) is 10 times higher than that of N_2 uptake (only 0.36 mmol g^{-1}), implying that the investigated carbons possess excellent selectivity for CO_2 adsorption. Based on the initial slopes of the CO_2 and N_2 adsorption isotherms, the CO_2-over-N_2 selectivity of NMC-600 reaches up to 50:1 at 25 °C (Fig. S6).[5, 6, 16] The excellent performance of NMC-*x* for CO_2 capture indicates that these carbons preferably interact with CO_2 molecules. It is well known that the kinetic diameter of CO_2 (0.33 nm) is smaller than that of N_2 (0.36-0.38 nm), and that CO_2 molecule has a larger electric quadrupole moment, arising from the strong dipolar C=O bonds, than N_2 molecule. Thus, the probable reasons for excellent CO_2 uptake may be (a) the large amount of uniform ultramicropores with the size of ca. 0.5 nm and (b) the polar surface caused by the heteroatom-containing (e.g. N, O, especially N) species. Note that this selectivity of CO_2-over-N_2 maybe decreases in practical CO_2 capture from flue gases due to the competitive adsorption of other gases in the flue gases, such as a few amount of O_2 and water vapor.

We also calculated the isosteric heat of adsorption (Q_{st}) by applying Clausius-Clapeyron equation to the CO_2 adsorption isotherms at 0 and 25 °C. As shown in Fig. 4d, NMC-600 exhibits the highest value of Q_{st}, indicating that this carbon strongly interacts with CO_2 molecules. The higher Q_{st} in the initial stage of adsorption leads to a selective adsorption of CO_2 over N_2 at low pressure for the NMC-*x*, which can be interpreted as (a) strong quadrupolar interactions of CO_2 molecules with the heterogeneous micropore walls (e.g., O/N-doped) and (b) strong adsorption potential of extremely small micropores. Finally, the regeneration of NMC-800 for CO_2 sorption at 25 °C is investigated. Clearly, the CO_2 sorption isotherms are almost completely reproducible (Fig. S7), indicating good regeneration stability of this carbon material for CO_2 uptake.

Conclusions

In summary, direct carbonization of K^+ exchanged meta-aminophenol-formaldehyde resin afforded a series of N-doped

microporous carbons with uniform ultramicropores (~0.50 nm). The NMC-*x* materials give very high CO_2 adsorption capacities at low partial pressure and impressive selectivity for CO_2 over N_2. We attribute these superior CO_2 sorption performances to the presence of both ultramicropores around 0.5 nm and N-doping.

We are grateful for the financial supports by Natural Science Foundation of China (NSFC51302156 and 21476264) and Distinguished Young Scientist Foundation of Shandong Province (JQ201215).

Notes and references

[a] School of Chemical Engineering, Shandong University of Technology, Zibo 255049, P. R. China. Tel. /fax: +86 533 2781664

[b] School of Science, State Key Laboratory of Heavy Oil Processing, China University of Petroleum Qingdao 266580 (P. R. China). Fax: (+) +86-533-86983579

[*]Corresponding author: S. Zhuo, E-mails: zhuosp_academic@yahoo.com W. Xing, E-mails: xingwei@upc.edu.cn

Electronic Supplementary Information (ESI) available: [details of any supplementary information available should be included here]. See DOI: 10.1039/c000000x/

1. D. W. Keith, *Science*, 2009, **325**, 1654-1655.
2. R. S. Haszeldine, *Science*, 2009, **325**, 1647-1652.
3. Y. Lee, D. Liu, D. Seoung, Z. Liu, C.-C. Kao and T. Vogt, *Journal of the American Chemical Society*, 2011, **133**, 1674-1677.
4. S. Keskin, T. M. van Heest and D. S. Sholl, *ChemSusChem*, 2010, **3**, 879-891.
5. J. An, S. J. Geib and N. L. Rosi, *Journal of the American Chemical Society*, 2009, **132**, 38-39.
6. R. Banerjee, H. Furukawa, D. Britt, C. Knobler, M. O'Keeffe and O. M. Yaghi, *Journal of the American Chemical Society*, 2009, **131**, 3875-3877.
7. N. P. Wickramaratne, J. Xu, M. Wang, L. Zhu, L. Dai and M. Jaroniec, *Chemistry of Materials*, 2014, **26**, 2820-2828.
8. Y. Zhang, B. Li, K. Williams, W. Y. Gao and S. Ma, *Chemical communications*, 2013, **49**, 10269-10271.
9. N. P. Wickramaratne and M. Jaroniec, *ACS applied materials & interfaces*, 2013, **5**, 1849-1855.
10. W. Xing, C. Liu, Z. Zhou, L. Zhang, J. Zhou, S. Zhuo, Z. Yan, H. Gao, G. Wang and S. Z. Qiao, *Energy & Environmental Science*, 2012, **5**, 7323-7327.
11. M. Sevilla and A. B. Fuertes, *Energy & Environmental Science*, 2011, **4**, 1765-1771.
12. X. Gao, X. Zou, H. Ma, S. Meng and G. Zhu, *Advanced materials*, 2014, **26**, 3644-3648.
13. N. P. Wickramaratne and M. Jaroniec, *Journal of Materials Chemistry A*, 2013, **1**, 112-126.
14. Z. Zhang, J. Zhou, W. Xing, Q. Xue, Z. Yan, S. Zhuo and S. Z. Qiao, *Physical Chemistry Chemical Physics*, 2013, **15**, 2523-2529.
15. Y. Zhao, L. Zhao, K. X. Yao, Y. Yang, Q. Zhang and Y. Han, *Journal of Materials Chemistry*, 2012, **22**, 19726-19731.
16. G. P. Hao, W. C. Li, D. Qian, G. H. Wang, W. P. Zhang, T. Zhang, A. Q. Wang, F. Schuth, H. J. Bongard and A. H. Lu, *Journal of the American Chemical Society*, 2011, **133**, 11378-11388.
17. G. Y. Gor, M. Thommes, K. A. Cychosz and A. V. Neimark, *Carbon*, 2012, **50**, 1583-1590.
18. M. Dubinin, *Carbon*, 1989, **27**, 457-467.
19. M. Sevilla, J. B. Parra and A. B. Fuertes, *ACS applied materials & interfaces*, 2013, **5**, 6360-6368.
20. A. Wahby, J. M. Ramos-Fernandez, M. Martinez-Escandell, A. Sepulveda-Escribano, J. Silvestre-Albero and F. Rodriguez-Reinoso, *ChemSusChem*, 2010, **3**, 974-981.
21. G. P. Hao, W. C. Li, D. Qian and A. H. Lu, *Advanced materials*, 2010, **22**, 853-857.
22. S. R. Caskey, A. G. Wong-Foy and A. J. Matzger, *Journal of the American Chemical Society*, 2008, **130**, 10870-10871.
23. K. L. Mulfort, O. K. Farha, C. D. Malliakas, M. G. Kanatzidis and J. T. Hupp, *Chemistry-A European Journal*, 2010, **16**, 276-281.
24. J. Wang, A. Heerwig, M. R. Lohe, M. Oschatz, L. Borchardt and S. Kaskel, *Journal of Materials Chemistry*, 2012, **22**, 13911-13913.
25. M. Sevilla and A. B. Fuertes, *Journal of Colloid Interface Science*, 2012, **366**, 147-154.
26. S. Y. Lee and S. J. Park, *Journal of colloid and interface science*, 2013, **389**, 230-235.
27. Q. Lin, T. Wu, S. T. Zheng, X. Bu and P. Feng, *Journal of the American Chemical Society*, 2012, **134**, 784-787.
28. G.-P. Hao, Z.-Y. Jin, Q. Sun, X.-Q. Zhang, J.-T. Zhang and A.-H. Lu, *Energy & Environmental Science*, 2013, **6**, 3740-3747.
29. M. Sevilla, P. Valle-Vigón and A. B. Fuertes, *Advanced Functional Materials*, 2011, **21**, 2781-2787.
30. Y. Xia, R. Mokaya, G. S. Walker and Y. Zhu, *Advanced Energy Materials*, 2011, **1**, 678-683.

